Tribology International 43 (2010) 1186–1192

Contents lists available at ScienceDirect

Tribology International

journal homepage: www.elsevier.com/locate/triboint

Feature based characterization of worn surfaces for a sliding test

Q. Hao [a,*], D. Bianchi [b], M. Kaestner [a], E. Reithmeier [a]

[a] Institute of Measurement and Automatic Control, Leibniz Universitaet Hannover, Nienburger Strasse 17, 30167 Hannover, Germany
[b] Austrian Center of Competence for Tribology, Viktor Kaplan Strasse 2, 2700 Wiener Neustadt, Austria

ARTICLE INFO

Available online 6 January 2010

Keywords:
Surface topography
Feature based characterization
Wavelet filter
Sliding test

ABSTRACT

In this paper a novel 3D surface characterization technique—feature based characterization—is applied to analyse worn surfaces from a ball on disc sliding test. This technique concentrates on analysis of surface features that are related to tribological behaviour. The worn surfaces of discs are segmented according to their surface texture primitives in order to analyse the shapes of the asperities. In order to remove shapes and unnecessary features of the ball surfaces, a filtering technique through wavelet analysis is applied. Then the significant features are extracted by means of a marker controlled watershed transformation. As a result, the relationship between the feature based parameters and the tribological behaviour is presented.

1. Introduction

The tribological behaviour of surfaces is dependent on materials, surface topographies, lubricants, external loads, relative motion, etc. Generally, the surface roughness has an influence on the tribological behaviour. Contrariwise, the wear process also influences the surface topography. The relationship between the 3D surface roughness parameters and the tribological behaviour has been well studied [1,2]. Functional 3D parameters have also been applied to investigate the tribological functionality of surfaces in forming processes and in engine systems [3,4]. Additionally, the 3D surface motif characterization techniques have been applied in tribology [5,6].

This paper presents an alternative surface characterization technique—feature based characterization—to investigate the topographies of worn surfaces. This technique can analyse the features of interest on the surface which can directly describe the tribological effects. A "ball on disc" sliding test was carried out where a ceramic ball was rubbed a steel disc. In the worn surface of the discs the typical textures caused by the abrasive wear can be seen. These surface textures could be interesting to investigate the wear mechanisms. Additionally, it is well known that the contact of two surfaces takes place at the peaks of the asperities [7]. Therefore there should be a relationship between the shape of asperities and the tribological behaviour. On the worn surfaces of the ceramic balls pit-like structures caused by brittle fracture occur on the surface. These pits may also relate to the wear and normal load.

A feature based characterization technique was published, which characterizes the surfaces according to their texture primitive [8]. This means, a surface can be divided into regions consisting of hills and regions consisting of valleys, like a landscape shown in Fig. 1. These regions consist of critical points (peaks, saddle points and pits). The boundaries between the hill regions are the course lines and the boundaries between the valley regions are the watershed lines. By using a Wolf pruning method [9] the information not relevant to the application can be removed. Then the surface is segmented according to the hill or valley regions.

A method for detecting particle and pore structures on a surface was also developed to characterize an AlSi cylinder liner surface [10]. By detecting the local maximal image gradient of the particles and pores and subsequent region merging, the particles and the pores on the surface can be extracted.

The aim of this work is to study the relationship of surface topography and tribological behaviour, such as friction and wear mechanisms, by analysing the features of the worn surfaces using the feature based characterization techniques.

2. Experimental details

2.1. Tribological test

A "ball on disc" tribometer was used for measuring the coefficients of friction of the surfaces under different load (Fig. 2). Three 100Cr6 steel disc samples with a calculated roughness of $S_a = 0.12\,\mu m$ were prepared through grinding. Al_2O_3 ceramic balls with nominal diameter of 10 mm were used as counterparts in the

* Corresponding author. Fax: +49 511/762 3234.
E-mail address: qiang.hao@imr.uni-hannover.de (Q. Hao).

0301-679X/$ - see front matter © 2010 Elsevier Ltd. All rights reserved.
doi:10.1016/j.triboint.2009.12.042

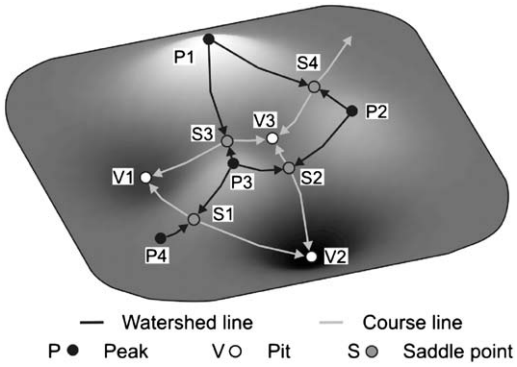

Fig. 1. Surface texture primitives.

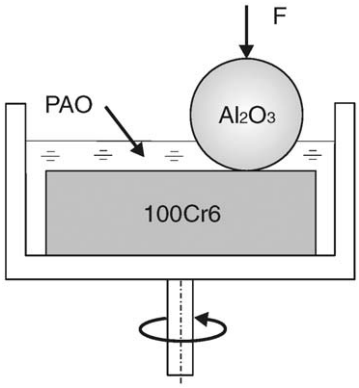

Fig. 2. Schematic of "ball on disc" sliding test.

test. The Vickers hardness of the ball is larger than 1500 HV and for the steel disc, it is about 700–800 HV. Three sliding tests were carried out under the same condition, varying the normal loads from 1 to 2 and 5 N. The coefficients of friction were monitored for a sliding distance of 50 m at the sliding speed of 0.05 m/s under lubricated condition (lubricant: pure PAO). Each test was carried out twice and the mean values of the coefficients of friction in the steady states under 1, 2 and 5 N are $0.162 \pm 4.2 \times 10^{-5}$, 0.152 ± 10^{-3} and $0.137 \pm 5.2 \times 10^{-4}$, respectively.

2.2. Topographical data acquisition

A white-light confocal microscope (μSurf from Nanofocus, Germany) was employed to acquire the topographical data of surfaces at the wear tracks. An objective with a numerical aperture (NA) of 0.8 was used in order to reduce the optical artefacts in the measuring results. The vertical and lateral resolutions for this objective are 2 and 312.5 nm, respectively according to Ref. [11].

The most common problem by optical measurements on rough surfaces is the "spike" artefact. It is very difficult to eliminate this artefact in the measuring results by using image processing. Normally this optical artefact can be reduced by using an objective with a higher numerical aperture. A roughness standard providing one dimension roughness was measured using the objective of 20× magnification (NA: 0.46) and 50× magnification (NA: 0.80) respectively. As shown in Fig. 3, the "spikes" are reduced in the measuring result by using an objective of 50× magnification.

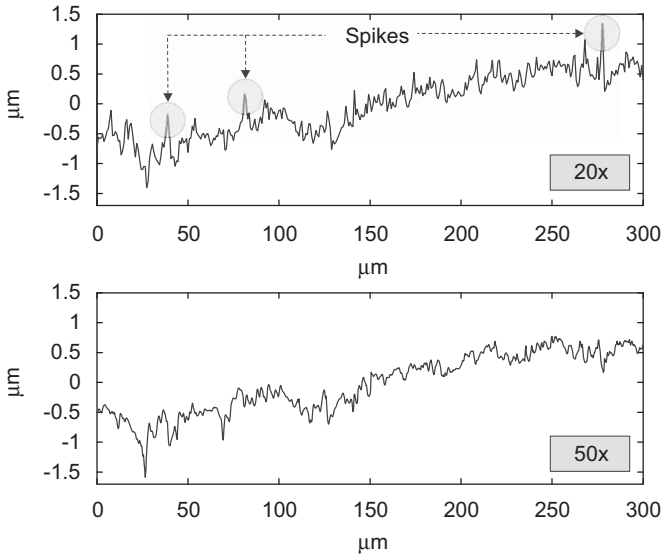

Fig. 3. Topography of a roughness standard measured with confocal microscope. Above: with objective of 20× magnification. Below: with objective of 50× magnification.

2.3. Surface characterization

2.3.1. Worn surfaces of the discs

The texture caused by the abrasive wear can give important information, such as the appearance of the worn surface and sliding direction, to the analyser. If the surfaces are considered as a landscape, then the texture will consist of a certain number of hill regions which show different shapes caused by the wear process. Therefore the feature of interest on the worn surfaces of discs is the texture, namely the hill region.

In order to characterize the hill regions of the surface, a segmentation of the surface is necessary. At first, the critical points (e.g. peak, pit and saddle point) are extracted according to the algorithms given in [12], after elimination of the form of the worn surface by using a Gaussian filter. Obviously not every hill region is significant for describing the surface features as it can be negligible in comparison of its neighbours. Therefore a method called "Wolf pruning" is employed to eliminate the insignificant hill regions. If the height difference between the saddle point and its neighbour peak in a hill region is below a certain threshold, then this peak will be considered as insignificant peak. After Wolf pruning, the surface is segmented by means of a marker controlled watershed transformation [13] where the remaining peaks are set as markers.

Fig. 4 shows the results of surface segmentation by varying the Wolf pruning threshold. Obviously, the use of different thresholds leads to different segmentation results. After using a threshold at 10 nm the hill features are so fine that they are not able to represent the characteristic of the worn surface. Contrariwise, after using a threshold at 50 nm some significant surface textures are not reflected in the segmentation result. The use of a threshold at 30 nm can lead to satisfying results. The feature based parameters for the worn surface under diverse normal load will be compared in this paper later, therefore the Wolf pruning thresholds are set for all worn surface at 30 nm. This means, that the hill regions, where the vertical difference between the peak and its nearest saddle point is smaller than 30 nm, are defined as insignificant structures. The feature based parameters has also been calculated by setting the threshold at 20 and 40 nm. The results show the same relationship between the parameters and the normal loads like by using a threshold at 30 nm.

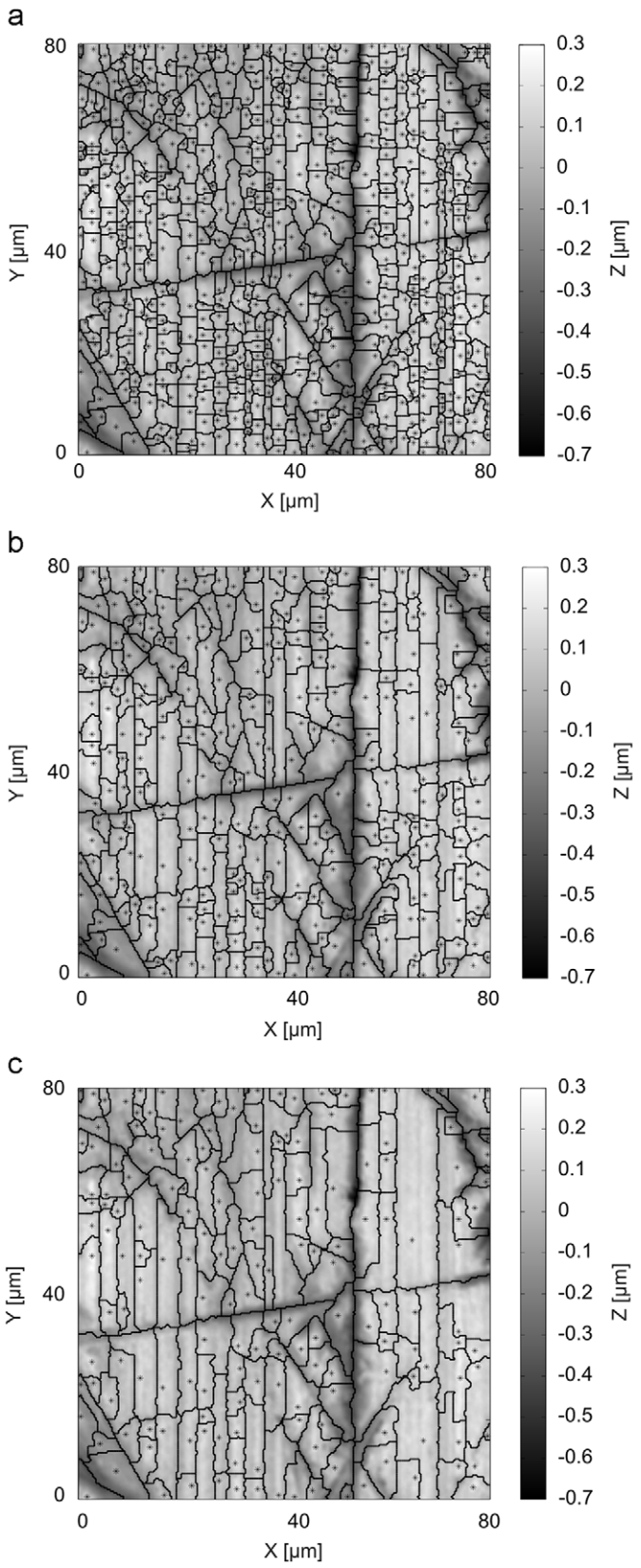

Fig. 4. Segmentation results of the surface at the wear track under a load of 5 N by using different Wolf Pruning thresholds: (a) 10 nm; (b) 30 nm; (c) 50 nm.

As Fig. 4b shows, each hill region is bordered by its course line and has a shape that is affected by the solid contact during sliding. In order to characterize the shapes of hill regions, the following feature based parameters are defined. One hill region is shown in Fig. 5.

The peak height (S_{ph}) is defined as the average difference between a peak and its course line. The hill area (S_{ha}) is the projected area of a hill region. The aspect ratio (S_{ar}) denotes the aspect ratio of a hill area in the sliding direction and is defined as the root of quotient of the sums of the distance square a_i^2 and b_i^2 [10] (see Fig. 6):

$$S_{ar}^2 = \frac{\sum_{i=1}^{n} a_i^2}{\sum_{i=1}^{n} b_i^2} \tag{1}$$

If the aspect ratio is small, it means the structure tends to have a longish form. Contrariwise, the structure tends to have a round form. The sliding direction can be approximated by calculating the position of the maximum of the curve which is obtained by smoothing the spectrum of orientation angle of hill regions (Fig. 7). The orientation angle is identified by fitting a line which passes the center of mass (S) of the hill area into the data points

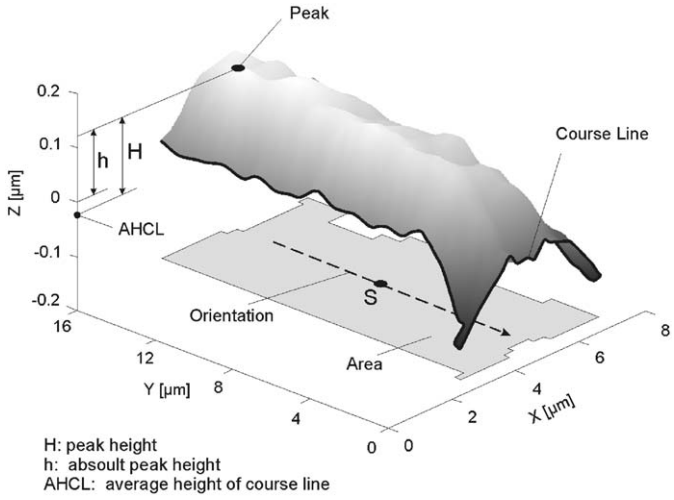

Fig. 5. Partial parameters for a hill region.

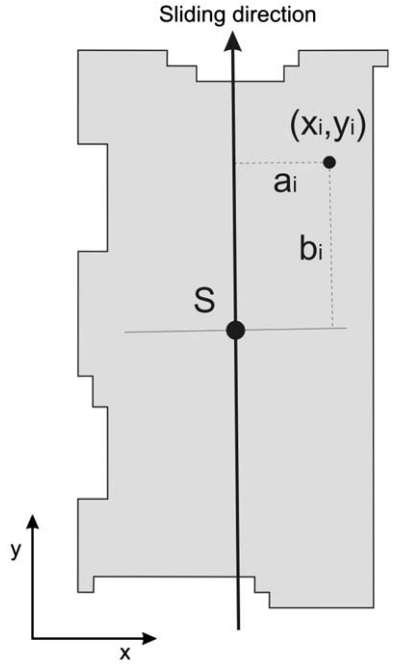

Fig. 6. Schematic of calculating the aspect ratio of a hill region.

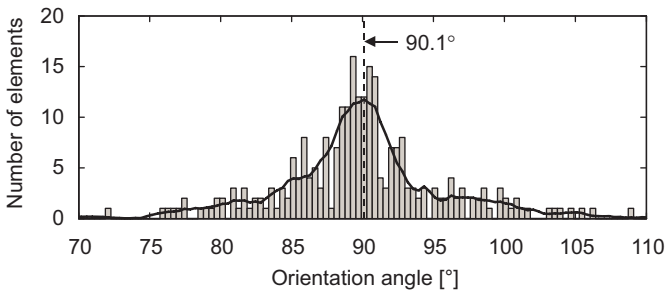

Fig. 7. Orientation angle spectrum of a worn surface under a load of 5 N.

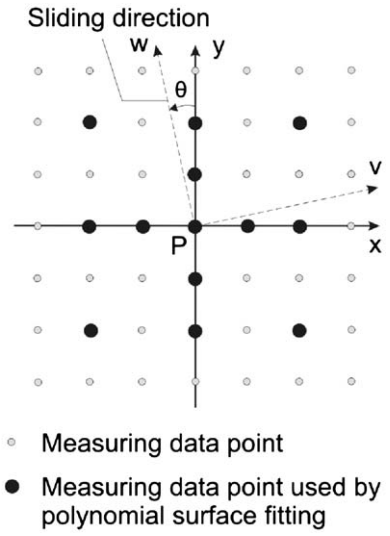

Fig. 8. Rotation of the measuring data points.

(x,y) (Fig. 6). The peak curvature indicates the value of the approximate peak curvature, which is obtained by a least square 2nd order polynomial surface formed by the surrounding points. The peak curvature in sliding direction (S_{pcs}) and the peak curvature in the perpendicular to the sliding direction (S_{pcps}) are designed to investigate the shapes of peaks in these directions. Larger peak curvature indicates a sharper shape of peak. In order to obtain the curvature of the fitted polynomial surface in the desired direction, the data is transformed into a new coordinate system (v,w) in which the direction of the w axis is parallel to the sliding direction (Fig. 8). The polynomial surface is defined as:

$$f(v,w) = a_{00} + a_{10}v + a_{01}w + a_{20}v^2 + a_{11}vw + a_{02}w^2 \quad (2)$$

Setting w to 0, the Eq. (2) can be formed as

$$f(v) = a_{00} + a_{10}v + a_{20}v^2 \quad (3)$$

The second derivative of $f(v)$ is defined as the peak curvature in the v direction:

$$f''(v) = |2a_{20}| \quad (4)$$

Similarly, the peak curvature in the w direction is

$$f''(w) = |2a_{02}| \quad (5)$$

The peak root mean square deviation (S_{pq}) denotes the root mean square deviation of the absolute peak height (see Fig. 5) in a sampling area. This parameter indicates the vertical distribution of peaks. The peak density (S_{pd}) is the number of the peaks in a unit area. This parameter describes the lateral distribution of peaks.

The parameters (S_{ph}, S_{ha}, S_{ar}, S_{pcs}, S_{pcps}) described above indicate the geometrical information of a single hill region. In order to represent the characteristic of the hill regions in a sampling area, the mean value of these parameters (mS_{ph}, mS_{ha}, mS_{ar}, mS_{pcs}, mS_{pcps}) is used.

2.3.2. Worn surface of the balls

Even though the Vickers hardness of the ceramic ball is about twice as large as the hardness of the steel disc, the wear of the ceramic ball is not negligible. Therefore, the surface topographies of the balls were also characterized. In Fig. 9 the pit-like structures can be observed on the worn surface of the ball in the wear zone clearly. Because the ceramic is a brittle material and the stress at asperity contact zones is high, the micro-cracks occur at the ceramic surface. The micro-cracks generate the chipping process so that the ceramic material breaks off from the surface [14]. Thus, the pit-like structures caused by the brittle fracture are formed on the ceramic surface. Therefore the pit can be considered as the feature of interest to analyse the relationship between the normal load and the abrasive wear of ceramics.

In order to characterize the pit area and volume, an algorithm [10] was applied for detecting the pits at the surfaces. At first the image gradient of surface is calculated. Then the topographical data points which lie under a setting threshold are assigned as markers. By using the marker controlled watershed transformation the surface can be segmented according to its local maximum of the image gradient. Finally the segments, which were marked before, are defined as pits.

Before applying the algorithm, for reducing possible artifacts error, a double filtering to the balls topography was applied. In the first step, for flattening the surface, a least square spherical surface was removed from the original image. In the second step, the surface roughness was removed through a wavelet filter [15] with a filtering threshold for the wavelet coefficient $T=0.5 \cdot S_a \cdot \sigma$, where S_a is the average amplitude of the surface, σ is the difference between the maximum and the minimum value of the flattened surface.

The result of pit detection in the wear zone under a load of 5 N is presented in Fig. 10.

Below, the feature based parameters designed to analyse the geometry of pits are summarized. The pit area (S_{pa}) and the pit volume (S_{pv}) are the area and the volume of a pit, respectively. For calculating the pit depth, the 95% pit depth ($S_{95\%pd}$) is used instead

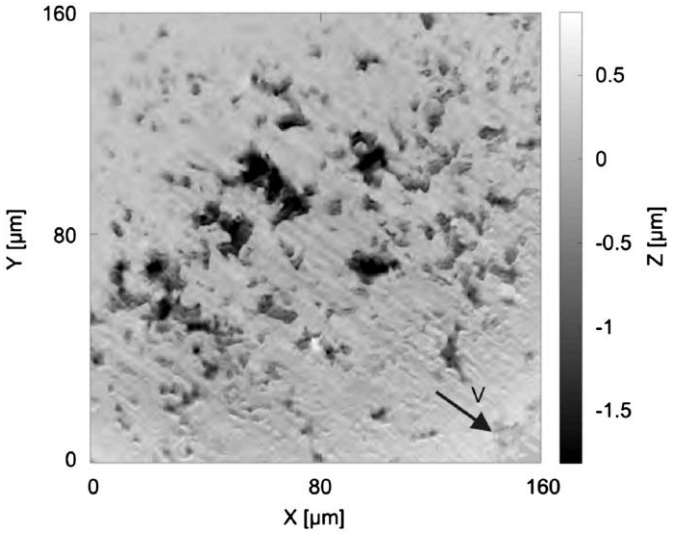

Fig. 9. Surface topography after an application of a wavelet filter in the wear zone under a load of 5 N in the steady state.

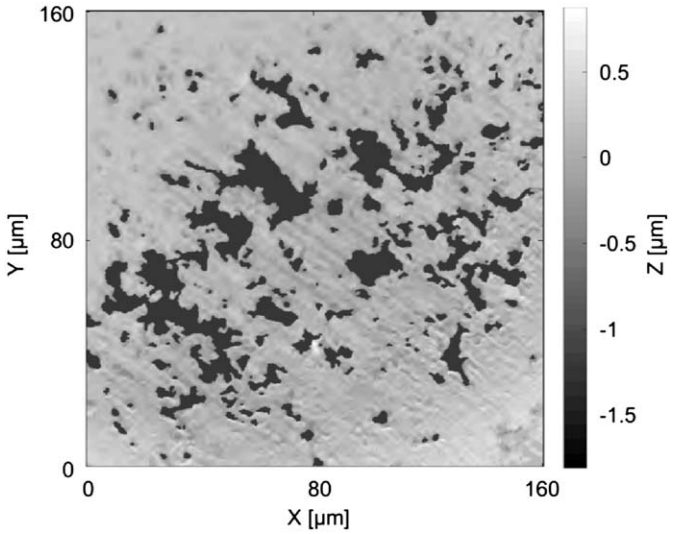

Fig. 10. Result of pit detection in the wear zone under a load of 5 N in the steady state.

Table 1
Comparison of the parameters of the surfaces at the wear tracks under different normal loads. (std: standard deviation).

Load	1 N		2 N		5 N	
	Mean	Std	Mean	Std	Mean	Std
mS_{ph} (μm)	0.189	0.011	0.186	0.016	0.178	0.010
mS_{ha} (μm^2)	23.26	2.20	22.95	2.83	20.42	1.87
mS_{ar}	0.479	0.014	0.460	0.023	0.441	0.016
mS_{pcs} (1/μm)	0.124	0.014	0.112	0.017	0.105	0.010
mS_{pcps} (1/μm)	0.241	0.016	0.260	0.019	0.295	0.017
S_{pq} (μm)	0.056	0.007	0.054	0.004	0.054	0.004
S_{pd} (1/μm^2)	0.039	0.004	0.040	0.004	0.045	0.004

of the maximum depth in order to increase the evaluation certainty for the optical measurement. $S_{95\%pd}$ represents the depth value after removing the lowest 5% values of one pit.

Like characterizing the hill regions, the mean value of the parameters (mS_{pa}, mS_{pv}, $mS_{95\%pd}$), described above for a single pit, is applied to generalize the topographical information of the pits in a sampling area. To describe the amount of the pit areas and the pit volumes, the total pit area (S_{tpa}) and the total pit volume (S_{tpv}) are also used here.

3. Results and discussion

3.1. Worn surfaces of the discs

The surface topographies were acquired in 10 positions at each wear track under different normal load and the respective mean values of the parameters, which have been presented in Section 2.3.1, are summarized in Table 1.

The lowest 15% of all peaks in a sampling area are assumed not to be in solid contact, because they may falsify the results of the evaluation. These regions are not taken into consideration by calculating the parameters. From Fig. 11, it can be seen that the decline of the curve of sorted peaks by the absolute height become faster in the last (lowest) 15% of the peaks. The statistic shows, that the invalid areas for all worn surfaces are smaller than 15% of the amount of peaks. For example, the invalid hill regions

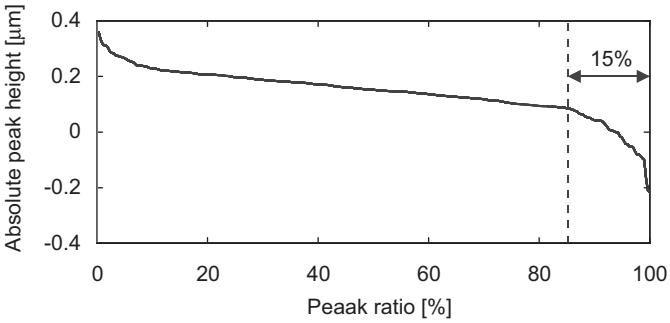

Fig. 11. Curve of sorted peaks for a worn surface under a normal load of 1 N.

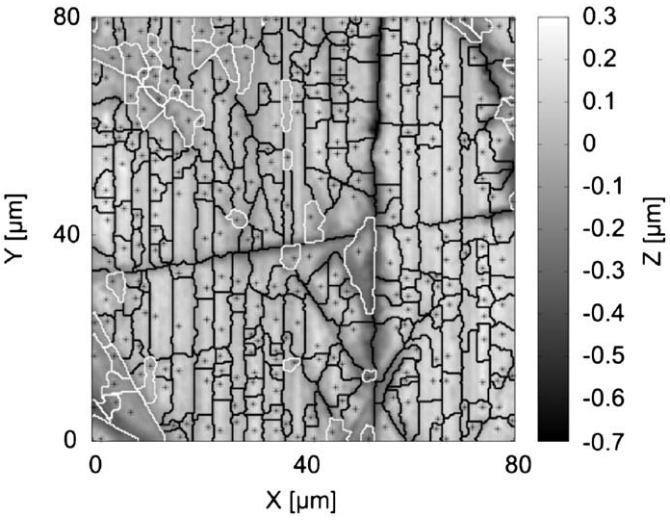

Fig. 12. Invalid hill regions (with white borders).

which are not considered in calculation of the parameters are shown in Fig. 12.

The values of mS_{ph} (mean peak height) and mS_{ha} (mean hill area) decrease with increased normal load. This shows that worn surfaces in the steady states tend to have finer structures with lower amplitude by increasing load. The values of mS_{ar} (mean aspect ratio) indicate that hill regions tend to have more longish structures by increased normal load in the sliding direction. The values of mS_{pcs} (mean peak curvature in sliding direction) decrease with the normal load. This shows that the shapes of peaks become blunter in the sliding direction by increasing load. Contrariwise, the values of mS_{pcps} (mean peak curvature in the perpendicular to the sliding direction) indicate that the shapes of the peaks are sharper in this direction with increased load. The differences between the values of S_{pq} (peak RMS deviation) are very small. The unevenness of the peaks of the worn surfaces may be independent of the normal load (at least in the range from 1 to 5 N). S_{pd} (peak density) for the surfaces under a load of 5 N is larger than it is for the surfaces under a load of 1 or 2 N. This indicates that more peaks occur on the surfaces under higher normal load.

As stated above, the shape of peaks in the sliding direction become blunter and the amount of peaks increases with the normal load. These may promote the decrease in friction during the sliding.

The conclusion shown above is based on analysing the mean values of parameters. Because of the amount of measurements (ten measurements for each sample), the standard deviation is about 10% of the mean values and sometimes makes the

differences of the mean values not very obvious, for example at the samples under the loads of 1 and 2 N. It can be expected that more significant results would be obtained by increasing the amount of measurements.

3.2. Worn surfaces of the balls

The values of parameters, which have been presented in Section 2.3.2, are calculated and the results are summarized in Table 2.

The values of S_{tpa} (total pit area) and S_{tpv} (total pit volume) show a clear relationship with the normal loads. This indicates that the amount of ceramic fragments, broken off from the surface, increases with the normal load. Increased ceramic debris, together with the steel wear debris, can give rise to the decrease in friction [7]. Even though the values of mS_{pa} (mean pit area), mS_{pv} (mean pit volume) and m$S_{95\%pd}$ (mean 95% pit depth) do not correlate with the normal load, it is worth investigating the "spectrum" of the areas and the volumes of pits. One of the advantages of the feature based characterization is that the geometrical information of each structure can be monitored. It gives a statistical result about the whole characteristic of features. In order to investigate the influence of the normal load on the pit sizes, the diagrams of pit areas versus pit volume are plotted in Fig. 13. The horizontal axis indicates the classes of pit areas and the vertical axis indicates the volume of the pits, which are assigned to their corresponding class of pit areas. The diagram shows that no pit, whose area exceeds 300 μm^2, occurs on the surface under the normal load of 1 N. By contrast, the pits with areas above 300 μm^2 are formed on the surface under a load of 2 and 5 N and their volumes also increase with the normal load.

The relationship between the pit area and its corresponding pit depth is presented in Figs. 14–16. The pits are sorted by their areas and numbered in ascending order. In order to have the same scale on the horizontal axes, the number of the pits divided by the total amount of pits is defined as the pit ratio. The upper diagrams of Figs. 14–16 show the sorted pit areas and the lower diagrams present their corresponding pit depths. The diagrams show a trend, that the pit depth rises with the increased pit area. This means, when the zones of chipping grow, the ceramic material breaks off deeper from the surface. In comparison to the worn surface under the normal load of 1 and 2 N, the pit depths at the worn surface under a normal load of 5 N increase abruptly at bigger pits. The reason may be that the micro-cracks occur deeper at the contact zones due to the increased stress so that the material removal process is favoured.

Table 2
Comparison of the parameters for the pore characterization of the ceramic balls in the wear zones under different normal loads.

Load	1 N	2 N	5 N
S_{tpa} (μm^2)	1989	2432	3839
S_{tpv} (μm^3)	1247	1465	3011
mS_{pa} (μm^2)	20.94	18.85	22.19
mS_{pv} (μm^3)	13.13	11.34	17.40
m$S_{95\%pd}$ (μm)	0.7626	0.6827	0.7811

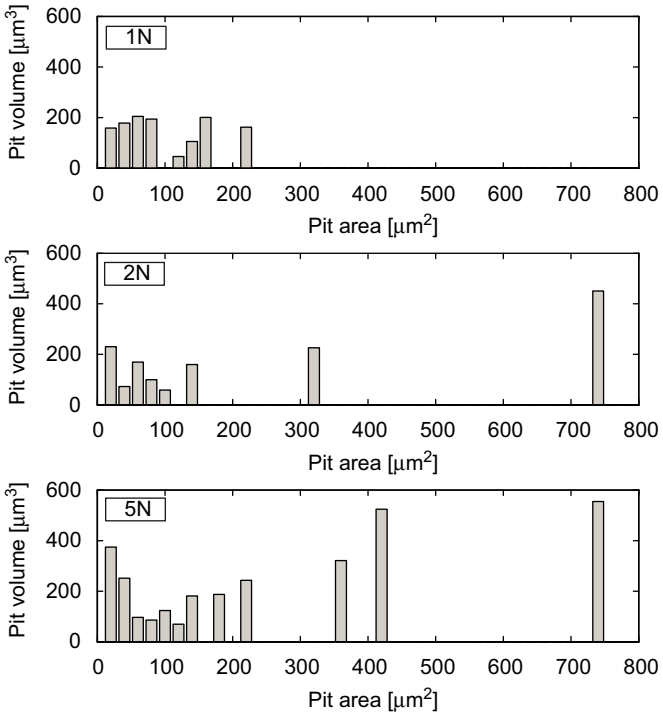

Fig. 13. Diagram of pit area vs. pit volume.

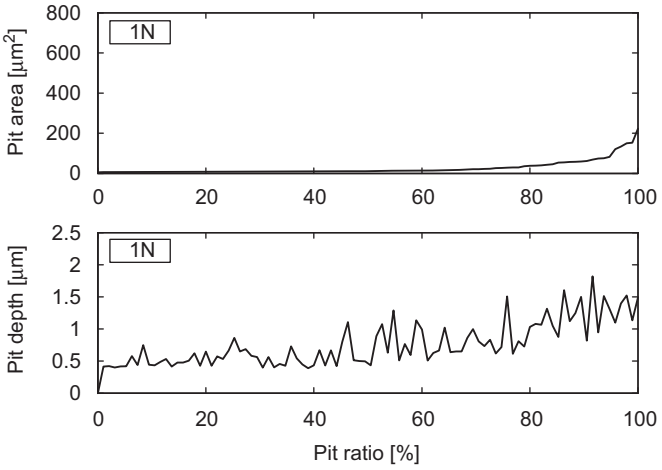

Fig. 14. Comparison of the spectrum of the pit depth under a normal load of 1 N.

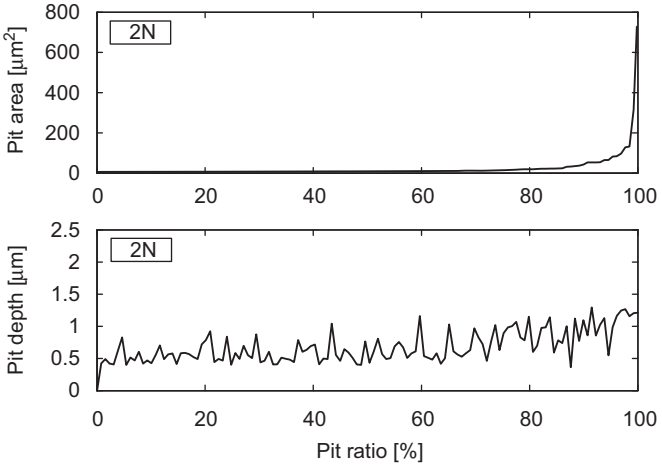

Fig. 15. Comparison of the spectrum of the pit depth under a normal load of 2 N.

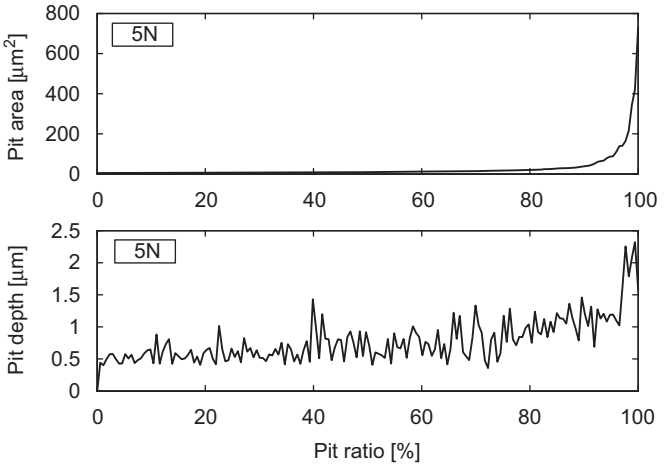

Fig. 16. Comparison of the spectrum of the pit depth under a normal load of 5 N.

4. Summary

The feature based characterization technique was applied to analyse two kinds of worn surfaces, both disc surfaces and ball surfaces, after the sliding tests. The feature based parameters can help the users to easily understand the geometrical information about the surface features such as hill regions on the surfaces of the steel discs and the pits on the ceramic balls. Most of the feature based parameters designed in this paper correlate with tribological behaviour.

In comparison to calculating the standard parameters, the computational efforts of the feature based characterization technique are larger and it also needs priori-knowledge about the surfaces. In addition, the definition of features is dependent on the analyser.

Acknowledgements

The authors would like to acknowledge the Centre for Tribology and Technical Diagnostics, University of Ljubljana, for supporting the experimental equipment and samples, and the project "WEMESURF", Marie Curie Researcher Training Network for the financial support. The personal support of Mr. Sedlacek for instructing the experiment is also acknowledged.

References

[1] Sedlacek M, Bodgornik B, Vizintin J. Influence of surface preparation on roughness parameters, friction and wear. ECOTRIB 2007;25: 784–94.
[2] Xiao L, Björgklund S, Rosen BG. Influence of surface roughness and the contact pressure distribution on friction in rolling/sliding contacts. Tribology International 2007;40:694–8.
[3] Weidel S, Engel U. Surface characterization in forming processes by functional 3D parameters. The International Journal of Advanced Manufacturing Technology 2007;33:130–6.
[4] Brinkmann S. Funktionsorientierte Beurteilung von Zylinderlaufflächen durch 3-dimensionale Oberflächenmesstechnik. Doctoral dissertation, Leibniz University of Hannover, 2002.
[5] Mezghani S, Zahouani H. Characterization of 3D waviness and roughness motifs. Wear 2004;257:1250–6.
[6] Zahouani H, Assoul M, Vargiolu R, Mathia T. The morphological tree transform of surface motifs-Incidence in tribology. International Journal of Machine Tools & Manufacture 2001;41:1961–79.
[7] Bhushan B. Principles and applications of tribology. Wiley; 1999 pp. 344–430.
[8] Scott PJ. Novel areal characterization techniques, advanced techniques for assessment surface topography. Kogan Page Science 2003: 43–62.
[9] Wolf GW. A Fortran subroutine for cartographic generalization. Computers and Geoscience 1991;17:1359–81.
[10] Weidner A. Strukturorientierte dreidimensionale Rauheitsauswertung von optisch vermessenen Zylinderlaufbahnen. Doctoral dissertation, Leibniz University of Hannover, 2006.
[11] NanoFocus AG. Handbook of µSurf. NanoFocus AG, Germany, 1st ed.; 2003. p. 9.
[12] Takahashi S, Ikeda T, Shinagawa Y, Kunni TL, Ueda M. Algorithms for extracting correct critical points and constructing topological graphs from discrete geographical elevation data. The International Journal of the Eurographics Association 1995;14:C181–92.
[13] Dougherty ER. The morphological approach to segmentation: the watershed transformation. In: Mathematical morphology in image processing. New York: Marcel Dekker Inc., 1993. p. 433–81 (Chapter 12).
[14] Ahn Y, Cho NG, Lee SH, Lee D. Lateral crack in abrasive wear of brittle materials. JSME International Journal, Series A 2003;46:140–4.
[15] Jiang XQ, Blunt L, Stout KJ. Lifting wavelet for three-dimensional surface analysis. International Journal of Machine Tools & Manufacture 2001;41:2163–9.